

RESIDUAL-STRAIN DETERMINATION BY LEAST-SQUARES REFINEMENT OF TOF NEUTRON-DIFFRACTION MEASUREMENTS OF DEFORMED URANIUM

N. C. Popa^{a,e}, D. Balzar^{b,c}, G. Stefanic^{b,c}, S. Vogel^d, D. Brown^d, M. Bourke^d, and B. Clausen^d

^aJoint Institute for Nuclear Research, Dubna, Moscow Region, Russia

^bDepartment of Physics and Astronomy, University of Denver, Denver, CO, USA

^cNational Institute of Standards and Technology, Boulder, CO, USA

^dLANSCE, Los Alamos National Laboratory, Los Alamos, NM, USA

^eNational Institute for Materials Physics, P.O.Box MG-7, Bucharest, Romania

ABSTRACT

We report the complete macroscopic average strain tensor for a cold-rolled uranium plate. The strain tensor was determined by the least-squares refinement of interplanar spacings for 19 Bragg reflections, as determined from the neutron TOF measurements at LANSCE. An annealed uranium plate was used as a reference sample, thus providing reference interplanar spacings for all 19 reflections. We also discuss the mathematical background for the calculation of the average macroscopic strain tensor as applied to the orthorhombic crystal symmetry and general triclinic sample symmetry of the uranium sample, based on a recently proposed method to determine texture-weighted strain orientation distribution function for arbitrary crystal and sample symmetries.

INTRODUCTION

A common procedure for the determination of residual strains is based on the directional measurements of the interplanar d spacings, the so-called $\sin^2\psi$ method [1]. An alternative approach was proposed [2, 3] that is based on the determination of strain and stress related parameters in Rietveld refinement [4]. In this way, both structure and microstructure (strain, stress, texture, and crystalline defects) information can be obtained simultaneously. In Rietveld refinement, all available Bragg reflections are used to obtain the strain tensor, which is of particular advantage in case of multiphase components and low crystalline symmetry systems with overlapping reflections. This procedure was successfully applied to the Al/SiC (short whisker) composites using GSAS program, which contains model for anisotropic strain correction for cubic or hexagonal symmetry [5]. A recently published model allows for accurate modeling of diffraction-line shifts in Rietveld-refinement for all Laue symmetries without making Voigt or Reuss approximation [6]. This is accomplished by expanding strain and stress tensor components in series of spherical harmonics, similarly to the texture modeling. The method yields the texture-weighted strain orientation distribution function (WSODF) and average macroscopic strain and stress tensors that are usually of engineering interest.

The aim here is to apply the methodology developed in the previous paper [6] to the neutron time-of-flight (TOF) measurements of two uranium samples in order to determine changes in the

This document was presented at the Denver X-ray Conference (DXC) on Applications of X-ray Analysis.

Sponsored by the International Centre for Diffraction Data (ICDD).

This document is provided by ICDD in cooperation with the authors and presenters of the DXC for the express purpose of educating the scientific community.

All copyrights for the document are retained by ICDD.

Usage is restricted for the purposes of education and scientific research.

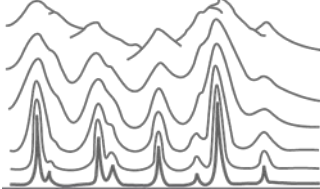
DXC Website

– www.dxcicdd.com

ICDD Website

- www.icdd.com

DENVER X-RAY CONFERENCE®



residual strain and stress state after plastic deformation. Uranium, a strategically important, although relatively poorly studied material, was chosen because of its orthorhombic crystalline structure (space group $Cmcm$, with unit-cell parameters at 25 °C: $a = 2.386 \text{ \AA}$, $b = 5.867 \text{ \AA}$, $c = 4.867 \text{ \AA}$).

THE MATHEMATICAL BACKGROUND

The strain calculated from the interplanar spacing of the sample under investigation (d) and the reference sample (d_0) is averaged through the rotation for ω around $\mathbf{h} = \mathbf{H}/H$ (\mathbf{H} being a reciprocal lattice vector for an (hkl) plane), which has to be parallel to \mathbf{y} , the direction of the diffraction vector in the sample:

$$\langle \varepsilon_{\mathbf{h}}(\mathbf{y}) \rangle = \langle d \rangle / d_0 - 1 \quad (1)$$

Following Popa & Balzar [6], the strain is given by the following equation:

$$\langle \varepsilon_{\mathbf{h}}(\mathbf{y}) \rangle P_{\mathbf{h}}(\mathbf{y}) = \sum_{l=0}^{\infty} \frac{2}{2l+1} I_l(\mathbf{h}, \mathbf{y}), \quad (2)$$

where the harmonic terms $I_l(\mathbf{h}, \mathbf{y})$ are defined below and the pole distribution functions

$$P_{\mathbf{h}}(\mathbf{y}) = (1/2\pi) \int_0^{2\pi} f(\varphi'_1, \Phi'_0, \varphi'_2) d\omega \quad (3)$$

can be used to calculate the crystallite orientation distribution function $f(\varphi_1, \Phi_0, \varphi_2)$. Here, $(\varphi_1, \Phi_0, \varphi_2)$ are the Euler's angles transforming the sample orthogonal coordinate system $(\mathbf{y}_1, \mathbf{y}_2, \mathbf{y}_3)$ into the crystallite orthogonal coordinate system $(\mathbf{x}_1, \mathbf{x}_2, \mathbf{x}_3)$,

The unit vectors of the directions in crystal and sample, \mathbf{h} and \mathbf{y} , are:

$$\mathbf{h} = A_1 \mathbf{x}_1 + A_2 \mathbf{x}_2 + A_3 \mathbf{x}_3 = \cos \beta \sin \Phi \mathbf{x}_1 + \sin \beta \sin \Phi \mathbf{x}_2 + \cos \Phi \mathbf{x}_3 \quad (4)$$

$$\mathbf{y} = \cos \gamma \sin \Psi \mathbf{y}_1 + \sin \gamma \sin \Psi \mathbf{y}_2 + \cos \Psi \mathbf{y}_3, \quad (5)$$

where (Φ, β) , (Ψ, γ) are the polar and azimuthal angles of \mathbf{h} and \mathbf{y} in their respective coordinate systems.

Depending on the crystalline and assumed sample symmetry, as well as on the strength and gradient of strain and texture, it is necessary to inspect (2) for a required number of terms to obtain the desired precision. We determined that for our sample the first three terms suffice:

$$\langle \varepsilon_{\mathbf{h}}(\mathbf{y}) \rangle P_{\mathbf{h}}(\mathbf{y}) = 2I_0(\mathbf{h}, \mathbf{y}) + \frac{2}{5} I_2(\mathbf{h}, \mathbf{y}) + \frac{2}{9} I_4(\mathbf{h}, \mathbf{y}) \quad (6)$$

The harmonic terms $I_l(\mathbf{h}, \mathbf{y})$ in (6) could be expressed in two different ways, depending on the purpose of investigation. If both macroscopic strain-stress tensors and WSODF are desired, the equations (17) to (20) from [6] must be used for any harmonic number l . But if only the macroscopic strain and stress tensors are needed, then a hybrid representation, that is, (17) to (20) for $l = 0, 2$ and (25), (26) for $l \geq 4$ are preferred because of a fewer number of parameters [6].

Thus, for orthorhombic crystal symmetry and triclinic sample symmetry, by using Tables 9 and 17 from [6], we obtain:

$$I_0 = A_1^2 t_{10} + A_2^2 t_{20} + A_3^2 t_{30}, \quad (7a)$$

$$t_{i0} = A_{i0}^0 P_0^0(\Phi), \quad A_{i0}^0 = \alpha_{i0}^{00} P_0^0(\Psi), \quad (i = 1,3) \quad (7b,c)$$

$$I_2 = A_1^2 t_{12} + A_2^2 t_{22} + A_3^2 t_{32} + 2A_2 A_3 t_{42} + 2A_1 A_3 t_{52} + 2A_1 A_2 t_{62} \quad (8a)$$

$$t_{i2} = A_{i2}^0 P_2^0(\Phi) + A_{i2}^2 \cos 2\beta P_2^2(\Phi), \quad (i = 1,3)$$

$$t_{42} = B_{42}^1 \sin \beta P_2^1(\Phi), \quad t_{52} = A_{52}^1 \cos \beta P_2^1(\Phi), \quad t_{62} = B_{62}^2 \cos 2\beta P_2^2(\Phi), \quad (8b)$$

$$A_{i2}^m = \alpha_{i2}^{m0} P_2^0(\Psi) + \sum_{n=1}^2 (\alpha_{i2}^{mn} \cos n\gamma + \beta_{i2}^{mn} \sin n\gamma) P_2^n(\Psi), \quad (i = 1,6)$$

$$B_{i2}^m = \gamma_{i2}^{m0} P_2^0(\Psi) + \sum_{n=1}^2 (\gamma_{i2}^{mn} \cos n\gamma + \delta_{i2}^{mn} \sin n\gamma) P_2^n(\Psi), \quad (i = 1,6), \quad (8c)$$

$$I_4 = M_{14} A_1^6 + M_{24} A_2^6 + M_{34} A_3^6 + M_{44} A_2^4 A_3^2 + M_{54} A_2^2 A_3^4 + M_{64} A_1^4 A_3^2 + M_{74} A_1^2 A_3^4 + M_{84} A_1^4 A_2^2 + M_{94} A_1^2 A_2^4 + M_{10,4} A_1^2 A_2^2 A_3^2, \quad (9a)$$

$$M_{k4} = \mu_{k4}^0 P_4^0(\Psi) + \sum_{n=1}^4 (\mu_{k4}^n \cos n\gamma + \nu_{k4}^n \sin n\gamma) P_4^n(\Psi), \quad (k = 1,10). \quad (9b)$$

The functions P_l^m were defined in [6]. The parameters α_{il}^{mn} , β_{il}^{mn} , γ_{il}^{mn} , δ_{il}^{mn} , μ_{kl}^n , ν_{kl}^n can be either determined by Rietveld refinement or solved for through a system of n linear equations. As this method of strain determination was not yet included in Rietveld refinement programs, we employed the latter approach. The parameters were determined by the least-square refinement by minimizing:

$$\chi^2 = (N - n)^{-1} \sum_{i=1}^N \left[\left(\langle \varepsilon_h(\mathbf{y}) \rangle P_h(\mathbf{y}) \right)_{im} - \left(\langle \varepsilon_h(\mathbf{y}) \rangle P_h(\mathbf{y}) \right)_{ic} \right]^2 / \sigma_i^2, \quad (10)$$

where N is the number of measured (m) points and n the number of free parameters. There are 3 parameters for $l = 0$, 45 for $l = 2$, and 90 parameters for $l = 4$, that is, 138 refinable parameters in total.

The macroscopic strain and stress tensors are obtained from the coefficients for $l = 0, 2$ by using the expressions (23) and (24) from [6]:

$$\bar{e}_i = \sum_{j=1}^6 \sum_{k=0}^{25} \bar{w}_{ijk} g_{jk} \quad (11)$$

$$\bar{s}_i = \sum_{j=1}^6 \sum_{k=0}^{25} \bar{w}_{ijk} g'_{jk}, \quad g'_{jk} = \sum_{l=1}^6 C_{jl} \rho_l g_{lk}. \quad (12a,b)$$

Here C_{jl} are the monocystal elastic stiffness modules; the matrix \mathbf{w} was given in Table 16 from [6]. For orthorhombic crystal symmetry and triclinic sample symmetry, the matrix \mathbf{g} and all 6 strain and stress components are given in [7]. Here, we give only expressions for the components of the strain tensor:

$$\begin{aligned}
 \bar{e}_1, \bar{e}_2 &= \frac{2}{3}\alpha_{10}^{00} + \frac{2}{3}\alpha_{20}^{00} + \frac{2}{3}\alpha_{30}^{00} + \frac{1}{15}\alpha_{12}^{00} + \frac{1}{15}\alpha_{22}^{00} - \frac{2}{15}\alpha_{32}^{00} \mp \frac{1}{30}\sqrt{\frac{3}{2}}\alpha_{12}^{02} \mp \frac{1}{30}\sqrt{\frac{3}{2}}\alpha_{22}^{02} \\
 &\pm \frac{1}{15}\sqrt{\frac{3}{2}}\alpha_{32}^{02} \pm \frac{1}{10}\alpha_{52}^{12} - \frac{1}{15}\sqrt{\frac{3}{2}}\gamma_{42}^{10} \pm \frac{1}{10}\gamma_{42}^{12} - \frac{1}{30}\sqrt{\frac{3}{2}}\alpha_{12}^{20} + \frac{1}{30}\sqrt{\frac{3}{2}}\alpha_{22}^{20} \pm \frac{1}{20}\alpha_{12}^{22} \\
 &\mp \frac{1}{20}\alpha_{22}^{22} - \frac{1}{15}\sqrt{\frac{3}{2}}\gamma_{62}^{20} \pm \frac{1}{10}\gamma_{62}^{22} \\
 \bar{e}_3 &= \frac{2}{3}\alpha_{10}^{00} + \frac{2}{3}\alpha_{20}^{00} + \frac{2}{3}\alpha_{30}^{00} - \frac{2}{15}\alpha_{12}^{00} - \frac{2}{15}\alpha_{22}^{00} + \frac{4}{15}\alpha_{32}^{00} + \frac{2}{15}\sqrt{\frac{3}{2}}\gamma_{42}^{10} \\
 &+ \frac{1}{15}\sqrt{\frac{3}{2}}\alpha_{12}^{20} - \frac{1}{15}\sqrt{\frac{3}{2}}\alpha_{22}^{20} + \frac{2}{15}\sqrt{\frac{3}{2}}\gamma_{62}^{20} \\
 \bar{e}_4 &= -\frac{1}{30}\sqrt{\frac{3}{2}}\beta_{12}^{01} - \frac{1}{30}\sqrt{\frac{3}{2}}\beta_{22}^{01} + \frac{1}{15}\sqrt{\frac{3}{2}}\beta_{32}^{01} + \frac{1}{60}\beta_{52}^{11} + \frac{1}{60}\delta_{42}^{11} + \frac{1}{20}\beta_{12}^{21} - \frac{1}{20}\beta_{22}^{21} + \frac{1}{10}\delta_{62}^{21} \\
 \bar{e}_5 &= -\frac{1}{30}\sqrt{\frac{3}{2}}\alpha_{12}^{01} - \frac{1}{30}\sqrt{\frac{3}{2}}\alpha_{22}^{01} + \frac{1}{15}\sqrt{\frac{3}{2}}\alpha_{32}^{01} + \frac{1}{60}\alpha_{52}^{11} + \frac{1}{60}\gamma_{42}^{11} + \frac{1}{20}\alpha_{12}^{21} - \frac{1}{20}\alpha_{22}^{21} + \frac{1}{10}\gamma_{62}^{21} \\
 \bar{e}_6 &= -\frac{1}{30}\sqrt{\frac{3}{2}}\beta_{12}^{02} - \frac{1}{30}\sqrt{\frac{3}{2}}\beta_{22}^{02} + \frac{1}{15}\sqrt{\frac{3}{2}}\beta_{32}^{02} + \frac{1}{10}\beta_{52}^{12} + \frac{1}{10}\delta_{42}^{12} + \frac{1}{20}\beta_{12}^{22} - \frac{1}{20}\beta_{22}^{22} + \frac{1}{10}\delta_{62}^{22}
 \end{aligned} \tag{13}$$

The sample volume change is given by the trace of the macroscopic strain tensor:

$$Tr(\bar{\mathbf{e}}) = \bar{e}_1 + \bar{e}_2 + \bar{e}_3 = 2(\alpha_{10}^{00} + \alpha_{20}^{00} + \alpha_{30}^{00}) \tag{14}$$

EXPERIMENT AND RESULTS

The neutron TOF diffraction experiments yield the whole diffraction pattern at every sample orientation. A comparable experiment with constant-wavelength neutrons or x-rays would require an order of magnitude longer data collection time in order to scan through several Bragg reflections to provide a sufficient number of d spacings to determine average strain and stress tensors by this method. The measurements were carried out at the Spectrometer for Materials Research at Temperature and Stress (SMARTS) at the Los Alamos Neutron Science Center (LANSCE), Los Alamos National Laboratory. The measurements were performed on two uranium plates (plastically deformed by cold rolling and annealed). The interplanar d spacings (neutron TOF measurements gave the information on 19 Bragg peaks) determined for the annealed plate were taken as the reference d_0 values at every sample orientation. Thus, the average macroscopic strain tensor reported here is relative to the state of strain in the annealed uranium plate. The samples were mounted in the Eulerian cradle with the χ circle fixed at 130° from the beam direction. We varied χ and ϕ angles to obtain 18 different sample orientations. By using four detector banks in the diffraction (horizontal) plane (at 98.4° , 81.6° , -98.4° and -81.6° 2θ), we obtained 72 histograms (diffraction patterns) at different sample angles. Texture was determined by GSAS, using the generalized spherical harmonics model [8]. (001) pole

figure for the rolled uranium sample is presented in Figure 1. It is evident that texture does not conform to mmm symmetry, as expected to be produced by rolling. Thus, we have not assumed either texture or strain sample symmetry in (6). Table 1 gives the full strain tensor, as determined from (13). As expected, there is a tensile strain in both rolling and transverse directions, about factor of four stronger for the former. This results in the compressive strain in the normal direction of about 10^{-4} . It is immediately noted that shear components are relatively strong. This may be caused by the slipping of rollers during cold rolling and/or significant texture present in the uranium plate before rolling was applied. However, a measurement yielding only strain components along principal sample axes, as it is customary carried out, would completely miss this information.

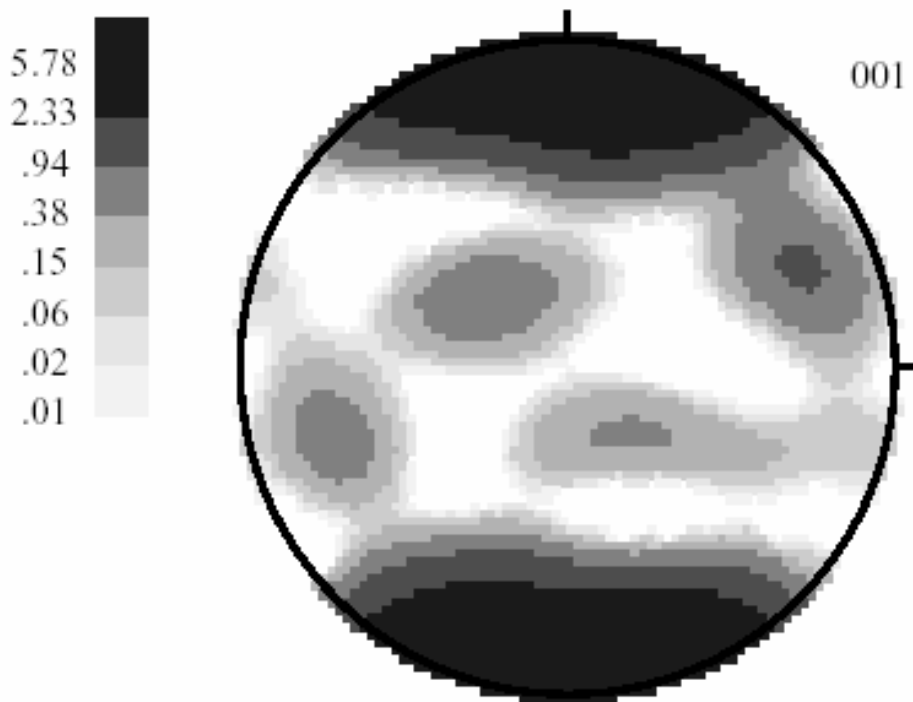


Figure 1. (001) pole figure for the cold-rolled uranium plate.

Table 1. Strain tensor in sample coordinates for a cold-rolled uranium plate, as determined from the neutron TOF measurements. The figure in parenthesis for \bar{e}_{11} gives standard uncertainty for the two least-significant digits, which is approximately constant for all strain-tensor components. \bar{e}_{22} - rolling direction, \bar{e}_{11} - transverse direction, \bar{e}_{33} - normal direction.

$$\bar{e} = \begin{pmatrix} 1.55(22) & -5.41 & -6.16 \\ -5.41 & 6.42 & -0.19 \\ -6.16 & -0.19 & -1.05 \end{pmatrix} \cdot 10^{-4}$$

CONCLUSION

In summary, we applied a recently developed model [6] for the determination of texture-weighted strain orientation distribution function to determine the average macroscopic strain tensor in cold rolled uranium plate. We presented a necessary methodology for an orthorhombic crystal symmetry and general triclinic sample symmetry and calculated all six components of the average strain tensor, based on the neutron TOF measurements collected at the SMARTS instrument at LANSCE. Strains are tensile in both rolling and transverse directions and compressive in the normal direction with strong shear components.

REFERENCES

- [1] Noyan, I. C. & Cohen, J. B., *Residual Stress, Measurement by Diffraction and Interpretation*. New York: Springer-Verlag, 1987.
- [2] Ferrari, M. & Lutterotti, L., *J. Appl. Phys.* **76** (1994) 7246-7255.
- [3] Balzar, D., Von Dreele, R. B., Bennett, K. & Ledbetter H., *J. Appl. Phys.* **84** (1998) 4822-4833.
- [4] Rietveld, H., *J. Appl. Cryst.* **2** (1969) 65-71.
- [5] Larson, A. C. & Von Dreele, R. B., *General Structure Analysis System GSAS*, Los Alamos National Laboratory Report, 2001.
- [6] Popa, N. C. & Balzar, D., *J. Appl Cryst.* **34** (2001) 187-195.
- [7] Balzar, D. *et al.*, in preparation.
- [8] Von Dreele, R. B., *J. Appl. Cryst.* **30** (1997) 517-525.